FEBS Letters 451 (1999) 152–156 FEBS 22033

Reconstruction of the dihydropyridine site in a non-L-type calcium channel: the role of the IS6 segment

Lubica Lacinová[1,*], Norbert Klugbauer, Min Hu, Franz Hofmann

Institut für Pharmakologie und Toxikologie, TU München, Biedersteiner Str. 29, 80802 Munich, Germany

Received 9 March 1999; received in revised form 9 April 1999

Abstract Mutations of eight to nine amino acids of IIIS5, IIIS6 and IVS6 segments were shown to reconstruct the dihydropyridine (DHP) interaction site in the non-L-type α_{1E} or α_{1A} calcium channels. The reconstructed site enabled enantiomer-selective inhibition and activation of the expressed chimeras by DHPs but failed to transfer voltage dependence of the current inhibition. Here we show that transfer of four non-conserved amino acids from the IS6 segment to the DHP-sensitive α_{1E} chimera increased the inhibition by (+)isradipine at the hyperpolarized membrane potential of −100 mV and enhanced the voltage-dependent block.

Key words: L-type calcium channel; Dihydropyridine binding site; Isradipine

1. Introduction

The α_{1C} subunit of the L-type calcium channel contains high affinity binding sites for organic channel blockers including the dihydropyridines (DHPs), phenylalkylamines and benzothiazepines (for review see [1]). Both native L-type calcium channels and the expressed α_{1C} subunit interact enantiomer-selectively with DHPs [2]. The affinity of the L-type calcium channel for the DHP enantiomers increases with depolarized membrane potential. This increase was attributed to the increased availability of the channel in the inactivated state [3–5].

The DHP sensitivity has been transferred successfully to the DHP-insensitive α_{1E} subunit [6] and α_{1A} subunit [7,8]. Mutation of two amino acid residues in IIIS5 (Y1295T, M1299Q), three residues in IIIS6 (F1406I, F1409I, V1414M) and three residues in IVS6 (I1706Y, F1707M, L1714I), yielding chimera rEC10 [6], allowed a high affinity interaction of the chimeric channel with isradipine at a holding potential (HP) of −100 mV. Sinnegger and coworkers [7] and Hockerman and coworkers [8], who additionally mutated M1713I in the IVS6 segment, reported results which did not differ from those of Ito and coworkers [6].

The reconstructed DHP site transferred enantiomer-selective activation and inhibition of the mutated channels by DHPs, but still lacked the characteristic voltage dependence of the inhibition. The cardiac and vascular splice variants of the L-type calcium channel are blocked with a different affinity by several DHPs [9–12]. Analyses of the structural backgrounds of this different sensitivity showed that the different sensitivity depended on the splice variant of the IS6 segment [13]. Therefore, we tested whether the transfer of amino acids from the IS6 segment could further improve the reconstructed DHP binding site. Here we report that transfer of four non-conserved amino acids from the IS6 segment of the α_{1C} subunit to the DHP-sensitive chimera rEC10 of the α_{1E} channel further decreased the IC_{50} for isradipine at a HP of −100 mV and enhanced the voltage dependence of the block.

2. Materials and methods

2.1. Construction of chimeric channels and cell transfection

In the chimera rEC10 eight amino acid residues of the α_{1E} sequence were replaced by corresponding amino acids of the α_{1C} sequence: Y1295T and M1299Q in IIIS5; F1406I, F1409I and V1414M in IIIS6; and I1706Y, F1707M and L1714I in IVS6. The construction of chimera rEC10 has been described in [6]. For the construction of rEC20, the *Kpn*I (nt 658)-*Xho*I (nt 1271) fragment of the rEC10 subunit [14] was subcloned in pUC18. Using a polymerase chain reaction overlap extension technique, the following mutations were made in the IS6 segment of the rEC10 sequence: N327P, L329I, I332V and P333T. These mutations were confirmed by sequence analysis in the subclone and in the full-length construct. The cDNAs for all chimeric constructs were cloned into the pcDNA 3 vector (Invitrogen). HEK 293 cells were transfected with the α_{1C-b} subunit [15] plasmids together with the cDNA plasmids encoding the cardiac β2a and $\alpha_2\delta$-1 subunits by lipofection with LipofectAMINE (Gibco BRL, Life Technologies) at a DNA mass ratio of 1:1:1.

2.2. Electrophysiological recording and data analysis

The whole cell Ba^{2+} currents were recorded using an EPC-9 amplifier (HEKA Elektronik GmbH, Lambrecht, Germany). The bath solution contained (in mM): NMDG, 125; $BaCl_2$, 20; CsCl, 5; $MgCl_2$, 1; EGTA, 0.1; HEPES, 10; glucose, 10; pH 7.4 (HCl). The intracellular solution contained (in mM): CsCl, 102; NaCl, 5; TEA-Cl, 10; EGTA, 10; MgATP, 5; HEPES, 5; pH 7.4 (CsOH). All chemicals were of the highest purity available. All experiments were carried out with the + enantiomer of isradipine. The stock solutions of isradipine was prepared in 96% ethanol, stored at −20°C and diluted to the required concentrations in the bath solution immediately before the experiment. Isradipine was applied by a local solution changer and reached the cell membrane within 1 s.

The capacity transient was compensated using the automatic procedure of the EPC-9 amplifier. Leak current was subtracted using the P/4 procedure. Data were analyzed by the program package provided by HEKA Elektronik and by Origin 4.0, Microcal Software Inc., Northampton, MA, USA. All values are means ± S.E.M.

3. Results and discussion

3.1. Voltage dependence of activation and inactivation of chimeric channels

For reconstruction of the DHP binding site, we chose the non-DHP-sensitive α_{1E} channel. The mutation of eight amino acids in the IIIS5, IIIS6 and IVS6 segments yielded the chi-

*Corresponding author. Fax: (49) (89) 4140 3261.
E-mail: lacinova@ipt.med.tu-muenchen.de

[1] On leave from the Institute of Molecular Physiology and Genetics, Slovak Academy of Sciences, Vlarska 5, 833 04 Bratislava, Slovakia.

PII: S0014-5793(99)00573-6

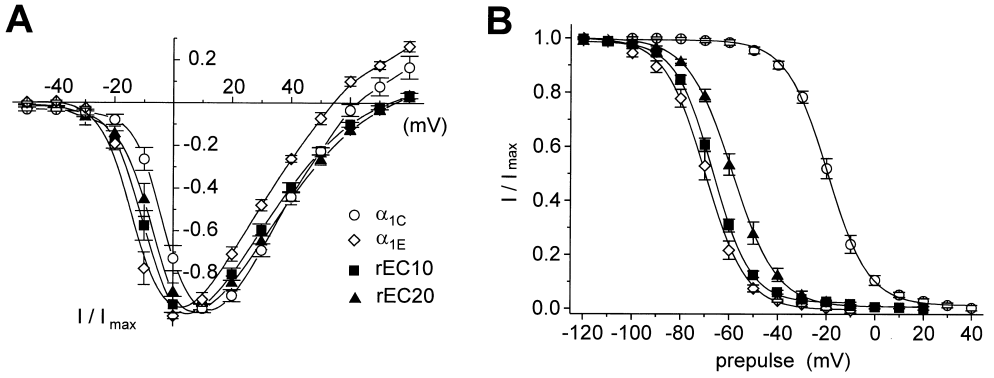

Fig. 1. A: *I-V* relations were measured by a sequence of 40 ms long pulses to the potentials between −50 mV and +80 mV applied each 5 s. HP was −80 mV for the α_{1C} channel (○) and −100 mV for the α_{1E} (◇), rEC10 (■) and rEC20 (▲) channels. Individual *I-V*s were normalized to the maximal inward current amplitude and then averaged. Solid lines are connectors of experimental points. B: Steady-state availability curves were measured by applying the following protocol each 20 s: the membrane potential was shifted from HP for 5 s to the prepulse voltage, returned to the HP for 5 ms, switched for 40 ms to the test potential which was equivalent to the peak *I-V* relation of each individual cell and returned to the HP. HP was −80 mV and prepulse voltages increased with a step +10 mV between −100 mV and +40 mV for the α_{1C} channel (○). For the α_{1E} (◇), rEC10 (■) and rEC20 (▲) channels, HP was −100 mV and prepulse voltages varied between −120 mV and +20 mV. Solid lines are fits of experimental data to the Boltzmann equation (see Table 1).

meric rEC10 channel which has an isradipine IC_{50} value of 57.5 ± 2.7 nM at a HP of −100 mV [6] (see also Fig. 2A). This IC_{50} value is 5-fold higher than that determined for the wild type α_{1C} channel, which was 12.2 ± 0.9 nM at a HP of −80 mV. In agreement with the α_{1A} chimeras [7,8], inhibition of the rEC10 chimera lacked voltage dependence of the DHP block. Obviously, DHP binding to the α_{1C} subunit requires additional, not yet identified amino acid(s). Analysis of the different DHP sensitivity of the cardiac and smooth muscle splice variants of L-type calcium channels pointed to a role of the IS6 segment in the high affinity interaction of the channels with DHPs [13].

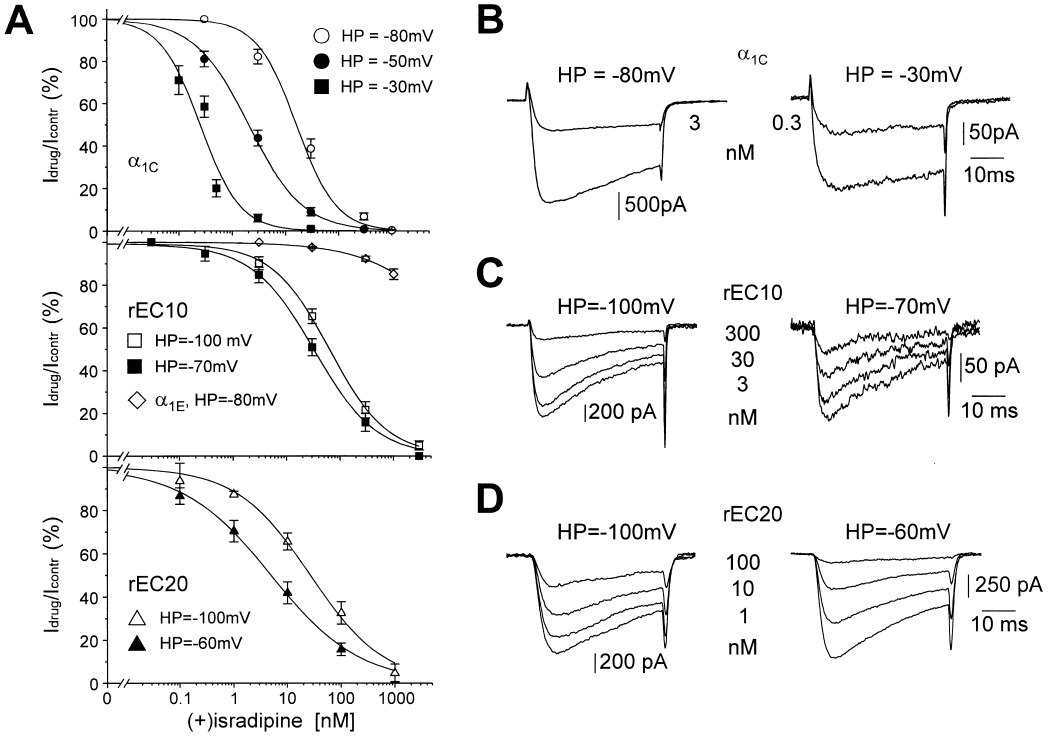

Fig. 2. A: Dose-response curves for inhibition of I_{Ba} by isradipine measured for the α_{1C} channel (upper panel) from HPs of −80 mV (○, $n=9$), −50 mV (●, $n=9$) and −30 mV (■, $n=8$); for the α_{1E} channel (middle panel) from HP of −80 mV (◇, $n=11$); for the rEC10 channel (middle panel) from HP of −100 mV (□, $n=7$) and −70 mV (■, $n=8$); for the rEC20 channel (lower panel) from a HP of −100 mV (△, $n=9$) and −60 mV (▲, $n=8$). Solid lines are fits of experimental data to the Hill equation (for resulting IC_{50}s see Table 2). B: Representative examples of current traces measured from α_{1C} channel at HPs of −80 mV and −30 mV in the absence and presence of 30 nM and 0.3 nM isradipine, respectively. C: Representative examples of current traces measured from the rEC10 channel at HPs of −100 mV and −70 mV in the absence and presence of 3, 30 and 300 nM isradipine (in order of descending amplitude). D: Representative examples of current traces measured from the rEC20 channel at HPs of −100 mV and −60 mV in the absence and presence of 1, 10 and 100 nM isradipine (in order of descending amplitude).

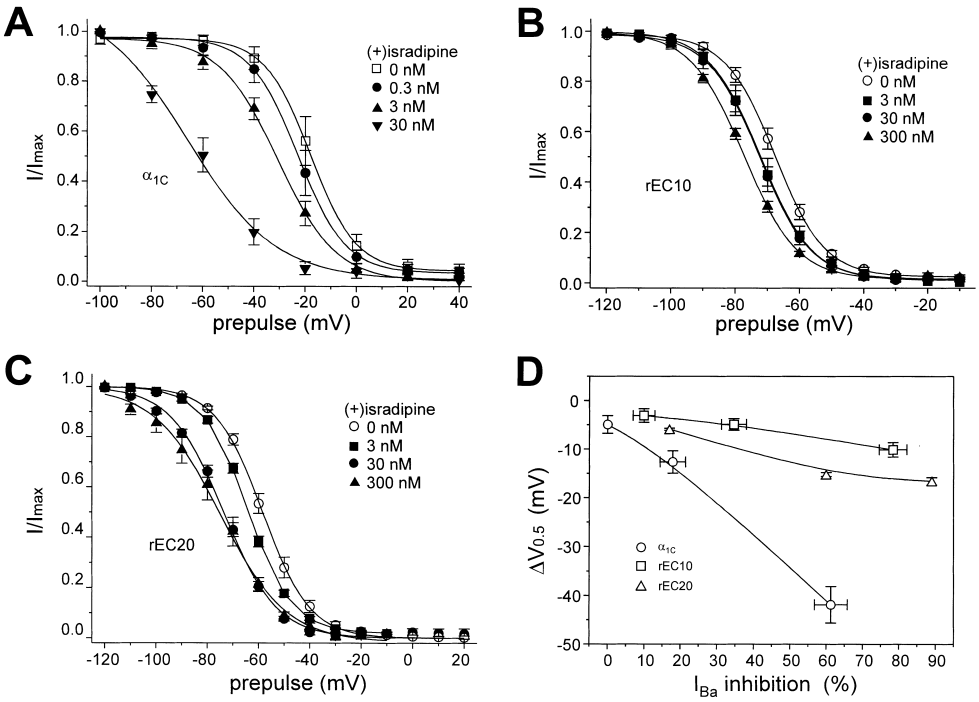

Fig. 3. Steady-state availability curves were measured as in Fig. 1 and fitted to the Boltzmann equation (solid lines in A–C). A: α_{1C} channel, HP of −80 mV, control conditions (□, $n=4$) and the presence of 0.3 nM (●, $n=4$), 3 nM (▲, $n=4$) and 30 nM (▼, $n=4$) isradipine. B: rEC10 channel, HP of −100 mV, control conditions (○, $n=8$) and the presence of 3 nM (■, $n=5$), 30 nM (●, $n=5$) and 300 nM (▲, $n=6$) isradipine. C: rEC20 channel, HP of −100 mV, control conditions (○, $n=7$) and the presence of 3 nM (■, $n=9$), 30 nM (●, $n=12$) and 300 nM (▲, $n=7$) isradipine. D: Relation between shift of voltage for half-maximal channel inactivation ($V_{0.5}$) and the inhibition of current amplitude by the same isradipine concentration. The x coordinate of each experimental point represents amplitude inhibition at an HP of −80 mV (α_{1C}, ○) or −100 mV (rEC10, □ or rEC20, △). Values are taken from experiments of Fig. 2A. The corresponding y coordinate represents shift of $V_{0.5}$ for steady-state availability by the same isradipine concentration. Values are taken from experiments in A–C.

To test this hypothesis, we mutated N327P, L329I, I332V and P333T of the IS6 segment of rEC10 chimera yielding chimera rEC20 (see Section 2). First, we characterized the voltage dependence of activation and inactivation of all used channels (Fig. 1). In comparison to the α_{1C} channel, the *I-V* relation of the α_{1E} channel was shifted by −10.8 mV (Table 1). The mutations of the rEC10 and rEC20 channels shifted the *I-V* relations towards the curve of the α_{1C} channel. In comparison to the α_{1C} channel, the quasi-steady-state inactivation curve of the α_{1E} channel was shifted by −50.1 mV (Table 1) and virtually overlapped with the quasi-steady-state inactivation curve of the rEC10 channel. The exchange of amino acids in the IS6 segment moved the voltage dependence of the inactivation of the rEC20 channels towards that of the α_{1C} channel.

3.2. Voltage dependence of current inhibition by isradipine

Inhibition of I_{Ba} by isradipine was tested by trains of 40 ms long depolarizing pulses to the membrane potential corresponding to the peak *I-V* relation of each individual cell. Two to three minutes were allowed at each drug concentration to establish new stable current amplitudes. The dose-response relations were established for all four channels (Fig. 2A). The DHP insensitivity of the α_{1E} channel was confirmed at HP −80 mV (Fig. 2A, middle panel). The DHP-sensitive channels were tested at hyperpolarized HP (−80 mV for the α_{1C} channel and −100 mV for the rEC10 and rEC20 channels), at which HPs the voltage-dependent inactivation of the channels is virtually zero, and at a depolarized membrane potential (−30 mV for the α_{1C} channel, −70 mV for the rEC10 and −60 mV for the rEC20 channels), at which HPs about 80% of

Table 1
Voltage-dependent activation and inactivation of individual channel types

	α_{1C}	α_{1E}	rEC10	rEC20
$V_{0.5act}$ (mV)	−4.3 ± 0.2	−15.1 ± 0.8	−11.7 ± 0.6	−9.1 ± 0.7
k_{act} (mV)	4.9 ± 0.1	3.5 ± 0.5	4.7 ± 0.6	4.9 ± 0.7
n	11	11	8	8
$V_{0.5inact}$ (mV)	−19.6 ± 0.3	−69.7 ± 0.4	−66.6 ± 0.1	−58.6 ± 0.2
k_{inact} (mV)	8.5 ± 0.2	8.4 ± 0.4	7.7 ± 0.1	9.1 ± 0.1
n	14	11	8	7

Values are the fits of the ascending part of *I-V* relations from Fig. 1A and of the steady-state availability curves from Fig. 1B to the Boltzmann equation. $V_{0.5act}$ and $V_{0.5inact}$ represent voltages for half-maximal activation and inactivation, respectively; k_{act} and k_{inact} are corresponding slope factors, n is number of cells tested.

Table 2
Voltage dependence of IC_{50} (nM) for inhibition of wild type α_{1C} and chimeric rEC10 and rEC20 channels by isradipine

HP (mV)	−100	−80	−70	−60	−50	−30
α_{1C}	–	16 ± 2	–	–	2.0 ± 0.3	0.25 ± 0.03
rEC10	64 ± 10	–	33 ± 7	–	–	–
rEC20	27 ± 4	–	–	5 ± 1	–	–

IC_{50} values for α_{1C}, rEC10 and rEC20 channels are results of fits of experimental data in Fig. 2A to the Hill equation. Holding potentials of −80 mV for α_{1C} and −100 mV for rEC10 and rEC20 channels represent membrane potentials at which virtually all channels were in a resting state. At holding potentials of −30 mV (α_{1C}), −70 mV (rEC10) and −60 mV (rEC20) about 80% of all channels were in an inactivated state.

the channels are inactivated. This extent of the voltage-dependent inactivation of the channels is greater than in quasi-steady-state inactivation curves showed in Fig. 1B because of the presence of an additional slow voltage-dependent inactivation which occurred in all channels. Apparently, complete steady-state inactivation curves would require at least a 1 min long prepulse. Nevertheless, a negative shift in the voltage dependence of the inactivation of individual channels was preserved. After a 5 s long prepulse, 80% of rEC10, rEC20 and α_{1C} channels were inactivated at approximate membrane potentials of −60 mV, −50 mV and −10 mV, respectively (see Fig. 1B). When the HP was shifted to a more depolarized value, 80% inactivation of rEC10, rEC20 and α_{1C} channels was reached at membrane potentials of about −70 mV, −60 mV and −30 mV, respectively. Therefore dose-response curves in Fig. 2A show inhibition of rEC10, rEC20 and α_{1C} channels under the conditions when the numbers of inactivated channels were approximately equal.

The differences in the voltage dependence of the isradipine interaction with individual channels is demonstrated also by examples of current traces recorded in the absence and the presence of isradipine. About the same extent of current inhibition was reached by 30 nM isradipine at an HP of −80 mV and by 0.3 nM isradipine at an HP of −30 mV in the wild type α_{1C} channel (Fig. 2B). Inhibition of the rEC10 channel by isradipine was similar at both HPs, i.e. at −100 mV and −70 mV (Fig. 2C). The shift of the HP from −100 mV to −60 mV enhanced the ability of isradipine to inhibit the rEC20 channel (Fig. 2D). All dose-response curves were fitted to the Hill equation. The voltage dependence of the IC_{50} values is summarized in Table 2. A shift in the membrane potential from −80 mV to −50 mV caused an 8-fold decrease in the IC_{50} for the wild type α_{1C} channel. A similar shift in the HP from −100 mV to −70 mV and −60 mV decreased the IC_{50} for the rEC10 channel only 1.9-fold and that for the rEC20 channel 5.4-fold. These values strongly support the hypothesis that the mutations of chimera rEC20 not only enhanced isradipine sensitivity of the channel at hyperpolarized membrane potential, but also contributed to the voltage dependence of the channel-drug interaction.

3.3. Shift of voltage dependence of channel availability by isradipine

Voltage-dependent interaction between the channel and a DHP is known to be accompanied by a shift in the voltage dependence of channel availability [5]. Therefore, we compared the ability of isradipine to shift the voltage dependence of channel availability (Fig. 3). In the wild type α_{1C} channel, isradipine induced a typical potent concentration-dependent shift of the availability curves towards more negative membrane potentials (Fig. 3A). In contrast, only a small shift was observed over a wide concentration range in the rEC10 channel (Fig. 3B). The ability of isradipine to shift the voltage dependence of channel availability was improved by the mutations of the rEC20 channel (Fig. 3C).

In the experiments shown in Fig. 3A–C, the isradipine concentrations used inhibited the current amplitude to different extents. Fig. 3D compares the voltage shift induced by a specific isradipine concentration with the extent of current inhibition caused by the same drug concentration. As expected, isradipine shifted the voltage of the inhibition curve strongly with increasing current inhibition if the wild type α_{1C} channel was used. This relation was very shallow for the rEC10 channel, but was improved in the rEC20 channel. These data document that the ability of isradipine to bind to and/or to stabilize the inactivated state of the channels also depends on amino acids of the IS6 segment.

In conclusion, we have demonstrated that amino acids of the IS6 segment of the calcium channel directly participate in forming the reconstructed DHP-interaction site in expressed DHP-insensitive α_{1E} and contribute to the voltage dependence of the interaction. These findings confirm the photoaffinity labeling data of Kalasz et al. [16] who reported that DHPs interact with amino acids of the IS6 segment. However, our results suggest also that high affinity interaction between the α_{1C} channel and DHPs requires additional parts of the channel. These may involve additional amino acids of IS6, IIIS5, IIIS6 and IVS6 segments, whose role in interaction with DHPs has not been identified yet, and/or amino acids of other transmembrane segments.

Acknowledgements: Supported by grants from the Deutsche Forschungsgemeinschaft and the Fonds der Chemie.

References

[1] Hofmann, F., Lacinová, L. and Klugbauer, N. (1999) Rev. Physiol. Biochem. Pharmacol. 139, 35–87.
[2] Triggle, D.J. (1991) J. Cardiovasc. Pharmacol. 18, (Suppl. 10) S1–S6.
[3] Bean, B.P. (1984) Proc. Natl. Acad. Sci. USA 81, 6388–6392.
[4] Hess, P., Lansman, J.B. and Tsien, R.W. (1984) Nature 311, 538–544.
[5] Sanguinetti, M.C. and Kass, R.S. (1984) Circ. Res. 55, 336–348.
[6] Ito, H., Klugbauer, N. and Hofmann, F. (1997) Mol. Pharmacol. 52, 735–740.
[7] Sinnegger, M.J., Wang, Z., Grabner, M., Hering, S., Striessnig, J., Glossmann, H. and Mitterdorfer, J. (1997) J. Biol. Chem. 272, 27686–27693.
[8] Hockerman, G.H., Peterson, B.Z., Sharp, E., Tanada, T.N., Scheuer, T. and Catterall, W.A. (1997) Proc. Natl. Acad. Sci. USA 94, 14906–14911.
[9] Welling, A., Kwan, Y.W., Bosse, E., Flockerzi, V., Hofmann, F. and Kass, R.S. (1993) Circ. Res. 73, 974–980.
[10] Hu, H. and Marban, E. (1998) Mol. Pharmacol. 53, 902–907.

[11] Zühlke, R.D., Bouron, A., Soldatov, N.M. and Reuter, H. (1998) FEBS Lett. 427, 220–224.
[12] Morel, N., Buryi, V., Feron, O., Gomez, J.P., Christen, M.O. and Godfraind, T. (1998) Br. J. Pharmacol. 125, 1005–1012.
[13] Welling, A., Ludwig, A., Zimmer, S., Klugbauer, N., Flockerzi, V. and Hofmann, F. (1997) Circ. Res. 81, 526–532.
[14] Schneider, T., Wei, X., Olcese, R., Costantin, J.L., Neely, A., Palade, P., Perez-Reyes, E., Qin, N., Zhou, J., Crawford, G.D., Smith, R.G., Appel, S.H., Stefani, E. and Birnbaumer, L. (1994) Receptors Channels 2, 255–270.
[15] Biel, M., Ruth, P., Bosse, E., Hullin, R., Stühmer, W., Flockerzi, V. and Hofmann, F. (1990) FEBS Lett. 269, 409–412.
[16] Kalasz, H., Watanabe, T., Yabana, H., Itagaki, K., Naito, K., Nakayama, H., Schwartz, A. and Vaghy, P.L. (1993) FEBS Lett. 331, 177–181.